

Dielectric and polarization switching anomalies near the morphotropic phase boundary in $\text{Pb}(\text{Zr}_{1-x}\text{Ti}_x)\text{O}_3$ ferroelectric thin films

Dongsun Sheen and Jong-Jean Kim*

Department of Physics, Korea Advanced Institute of Science and Technology, Taejeon, 305-701, Korea
(Received 12 September 2002; revised manuscript received 15 November 2002; published 4 April 2003)

Dielectric constants (ϵ' , ϵ'') and switching current transients of $\text{Pb}(\text{Zr}_{1-x}\text{Ti}_x)\text{O}_3$ thin films are measured for mixing concentrations of $x=0.46$, 0.48 , and 0.49 in the morphotropic phase boundary (MPB) region as a function of temperature from 80 K to 600 K. Anomalies in ϵ' and ϵ'' are observed in the measuring frequency range of 10 Hz to 100 KHz. The anomalies exhibiting a frequency dispersion tend to a low-temperature phase transition. The MPB transition temperatures for $x=0.46$, 0.48 , and 0.49 are located at ~ 490 K, ~ 325 K, and ~ 235 K, respectively, by dielectric measurements at 50 kHz. We have found that a frequency dispersion in the peak anomaly of ϵ'' associated with the MPB transition may be represented by Vogel-Fulcher law with a finite freezing temperature. The freezing temperatures are obtained as 309.6 K, 194.9 K, and 182.2 K for $x=0.46$, 0.48 , and 0.49 , respectively. It is suggested that the frequency dispersion between the MPB transition and the freezing temperature may be ascribed to a coexistence between tetragonal and monoclinic (or rhombohedral) phases. The switching current transients measured at different driving fields and fitted to the Ishibashi model characterize well a low-dimensional nature of the lead zirconate titanate (PZT) thin films in the domain dynamics. We have found that the maximum switching current density in the infinite field limit exhibits a plateau dependence across the MPB transition, which reflects a polarization saturation. The reduction of activation fields observed in the MPB transition may be caused by increasing random competitions of phase coexistence leading to local fluctuations of polar directions near the MPB. These results conform with the low-temperature phase transitions in the PZT thin films of the MPB concentration.

DOI: 10.1103/PhysRevB.67.144102

PACS number(s): 77.80.Bh, 64.70.Kb, 85.50.Gk

I. INTRODUCTION

The lead zirconate titanate thin-film system $\text{Pb}(\text{Zr}_{1-x}\text{Ti}_x)\text{O}_3$ (PZT) is one of the most attractive perovskite materials for microstructured ferroelectric devices. In general, a morphotropic phase boundary (MPB) of the PZT system separates the Ti-rich tetragonal phase (space group $P4mm$) from the Zr-rich rhombohedral phase ($R3m$ or $R3c$). Electromechanical and dielectric susceptibilities are known to exhibit the maximum at the rhombohedral side close to the MPB in Pb containing perovskite oxides such as PZT, $\text{Pb}(\text{Zn}_{1/3}\text{Nb}_{2/3})\text{O}_3$ - $x\text{PbTiO}_3$ (PZN-PT), $\text{Pb}(\text{Mg}_{1/3}\text{Nb}_{2/3})\text{O}_3$ - $x\text{PbTiO}_3$ (PMN-PT), etc. Additionally, a recent observation of a very large piezoelectricity in a rhombohedral-structured PZN-PT single crystal poled in the $[001]$ direction¹ has revived interest in the phase transition at the MPB.²⁻⁴ To manifest this phase transition in the PZT system is not easy because of the lack of a single crystal and the steepness of the MPB in the x - T phase diagram. For PZT ceramics, the studies on the phase transition near the MPB have been carried out by measuring the temperature dependencies of x-ray-diffraction (XRD) peaks, real parts of dielectric constants, electromechanical coefficients, Raman modes, etc.⁵⁻⁹ The results confirm the existence of a phase transition at the MPB in the PZT ceramics although the nature of the phase transition is unclear. Recently, a monoclinic phase (space group Cm) has been suggested from both fine XRD studies of PZT ceramics^{10,11} and first-principles calculations of a PZT cell structure¹² as a buffered phase between the tetragonal and rhombohedral phases near the MPB ($0.45 \leq x \leq 0.52$). It is also known that tetragonal and rhom-

bohedral (or monoclinic) phases can coexist near the MPB in the PZT system.^{4,5} Several works suggest a region of phase coexistence in PZT ceramics.^{7,11,13} Compared with the number of PZT ceramics studies, only a few studies related to the phase transition at the MPB for the PZT thin films have been reported in spite of the tremendous technical importance of thin films.

In this work, we present the temperature dependencies of dielectric responses and polarization reversal properties in the $\text{Pb}(\text{Zr}_{1-x}\text{Ti}_x)\text{O}_3$ thin films near the MPB. The results show that both real and imaginary parts of the dielectric constants have anomalies of frequency dispersions near the MPB. These anomalies can be described by a Vogel-Fulcher law with a finite freezing temperature. A correspondence between the frequency dispersion region and the phase coexistence region is shown. From the analysis of switching current transients, we have found that the maximum switching current density in the infinite field limit and thus the activation field exhibit anomalies near the MPB in the PZT thin-film system. These anomalies depict a precursory temperature dependence toward the low-temperature phase transition at the MPB concentration.

II. EXPERIMENT

PZT thin films of different compositions were prepared by a conventional sol-gel process. PZT thin films on Pt(111)/ TiO_2 / SiO_2 /Si substrates were deposited by spin coating a PZT solution with excess lead by 10 mol %. For pyrolysis the thin films were dried at 450 °C for 10 min on a hot plate. The thin films were treated by thermal annealing at 650 °C for 30 min in an ambient oxygen for the perovskite crystallization with (111) orientation. The $\text{Pb}(\text{Zr}_{1-x}\text{Ti}_x)\text{O}_3$

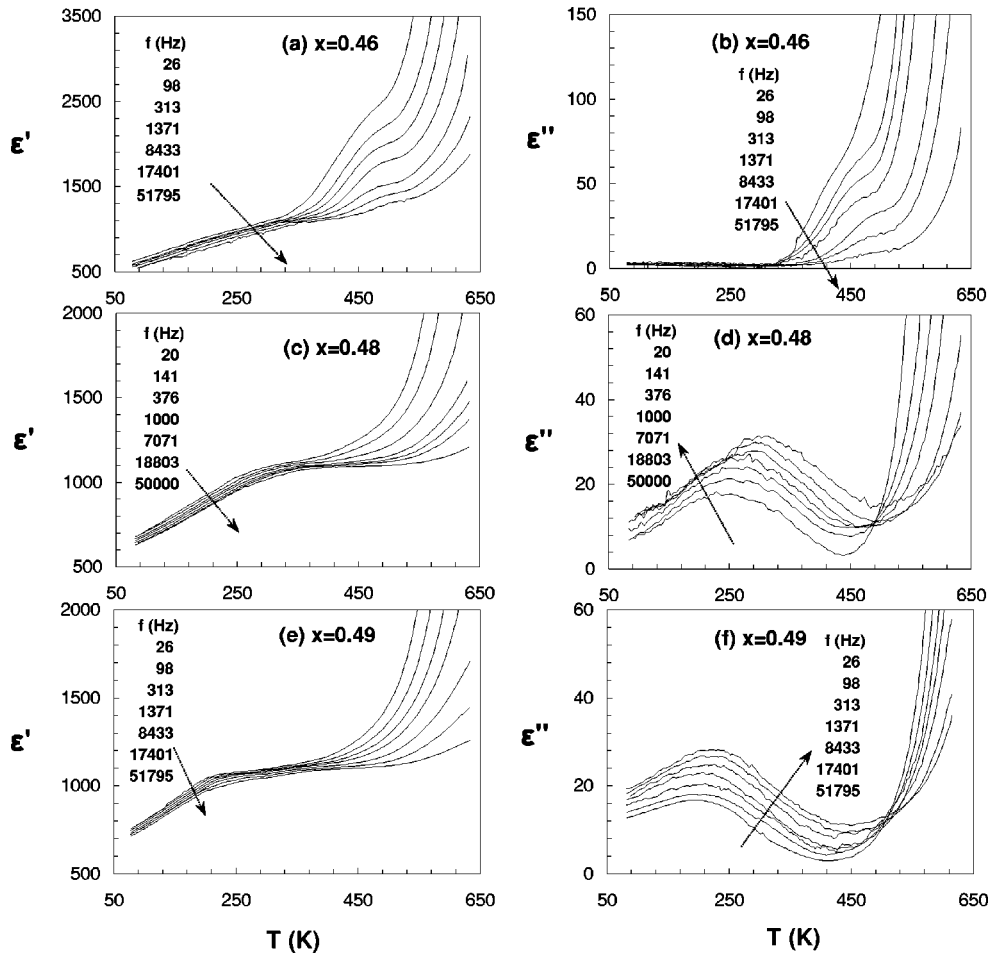


FIG. 1. Temperature and frequency dependencies of dielectric constants ϵ' and ϵ'' in $\text{Pb}(\text{Zr}_{1-x}\text{Ti}_x)\text{O}_3$ thin films for (a) and (b) $x=0.46$ (c) and (d) $x=0.48$ and (e) and (f) $x=0.49$ real part ϵ' in (a), (c), and (e) and imaginary part ϵ'' in (b), (d), and (f). Arrows guide for corresponding dielectric data curves in the directions of increasing frequency.

thin films used in the present study were about 250-nm thick with compositions of $x=0.46$, 0.48, and 0.49. Thickness of the thin films was confirmed by a surface profiler. Platinum dots were sputtered onto the PZT thin films for top electrodes to form capacitors. The area of each capacitor was about $4.9 \times 10^{-4} \text{ cm}^2$. The PZT capacitors were annealed at 650°C for 30 min in ambient oxygen to provide for improved contact by suppressing interface defects between a top electrode and PZT thin-film.

In order to study temperature dependence of electrical properties of the PZT thin film capacitors, a sealed pin probe method was employed. By employing this method with a Linkam heating stage, samples could be isolated from external disturbance during electrical measurements. Temperature was controlled in the range of 80 K to 600 K using a temperature controller and a liquid-nitrogen supplier. All electrical measurements were performed after temperature was stabilized. The dielectric constant measurements were carried out in the frequency range of 10 Hz to 100 kHz with amplitude of $0.08 V_{rms}$ using a lock-in amplifier (EG&G model DSP7260) and a standard capacitor. The capacitance of the standard capacitor was sufficiently larger than those of the PZT thin-film capacitors. Real (ϵ') and imaginary (ϵ'') parts

of the complex dielectric constants were measured simultaneously. Switching current transients were measured by use of a digital oscilloscope, a wave-form function generator and a small standard resistor. Only one set of square pulses was programmed by the function generator and applied on the samples to avoid a fatigue effect of the PZT thin films. A set of square pulses was constructed by combining two positive square pulses and two negative square pulses in series. Pulses were separated by 2-msec each with amplitudes between 0.5 and 9.0 V. A full current pulse and a nonswitching current pulse were derived from the pulses of opposite polarity and the pulses of same polarity, respectively. A true switching current transient, which is almost free from the circuit conditions, was then obtained by subtracting the nonswitching current from the full current pulse.

III. RESULTS AND DISCUSSION

A. Dielectric responses

Both ϵ' and imaginary ϵ'' parts of the dielectric constants of $\text{Pb}(\text{Zr}_{1-x}\text{Ti}_x)\text{O}_3$ thin films for $x=0.46$, 0.48, and 0.49 are shown in Fig. 1 as a function of temperature at varying fre-

quencies. The data were obtained in the cooling process. Approaching the Curie temperature (T_C) ~ 660 K of the ferroelectric phase transition, ϵ'' as well as ϵ' rapidly increase with decreasing frequency, imply that conductivity of thin films may increase rapidly at high temperatures. The columnar grain boundaries of polycrystalline thin films can provide a current path for mobile charges at high temperatures. As temperature decreases from T_C , all the PZT thin films used in the present study were expected to reach the morphotropic phase boundary. We have seen that anomalies not only in ϵ' but also in ϵ'' exist at a lower temperature than the Curie temperature. Both ϵ' and ϵ'' exhibit a shoulder and a small peak anomaly at each frequency, respectively, at a low temperature (T_L) dependent on the mixing compositions. These anomalies move to lower temperatures as the mixing concentration (x) increases. The anomalies exhibit frequency dispersions for all the three compositions. At lower frequencies, the anomalies in both ϵ' and ϵ'' shift to lower temperatures. In fact, the frequency dependence of small peaks in ϵ'' has not been reported in previous MPB studies of PZT ceramics, whereas similar anomalies near the MPB have been observed by Schmidt *et al.*¹⁴ in dielectric constant measurements of a $[\text{PMN}]_{0.66}[\text{PT}]_{0.33}$ single-crystal system.

This low-temperature anomaly may indicate the presence of a phase transition near the MPB. This phase transition of the $\text{Pb}(\text{Zr}_{1-x}\text{Ti}_x)\text{O}_3$ system with $x=0.46$, 0.48 , and 0.49 implies a change from a tetragonal to a monoclinic symmetry with decreasing temperature. The MPB transition temperatures (T_L) for $x=0.46$, 0.48 , and 0.49 may be assigned as ~ 490 K, ~ 325 K, and ~ 235 K, respectively, by the high-frequency (50 kHz) dielectric measurements (see Appendix A). The result is consistent with previous suggestions^{5,7,11} regarding PZT ceramics. Considering frequency dispersions with anomalies in both ϵ' and ϵ'' , this phase transition may well belong to a diffuse phase transition. The frequency-dependent anomalies in both ϵ' and ϵ'' can be also evidence of a phase coexistence near the MPB.

The frequency dispersion in the imaginary part (ϵ'') of dielectric constants can be described by a superposition of Debye relaxors with varying relaxation times τ ,

$$\epsilon''(\omega, T) = \epsilon_0(T) \int_0^\infty g(\tau, T) \frac{d(\omega\tau)}{1 + \omega^2\tau^2}, \quad (1)$$

where $g(\tau, T)$ is a distribution function^{15,16} of relaxation times τ and the normalization is given by $\int_0^\infty g(\tau, T) d(\ln \tau) = 1$. The frequency dispersion in ϵ'' is also characterized by a Vogel-Fulcher law,

$$\nu_c = \nu_0 \exp\left(-\frac{U_c}{T-T_0}\right), \quad (2)$$

where $\nu_c = \omega/2\pi$ is a cutoff frequency and ϵ'' shows a maximum peak at measuring temperature T , U_c is activation energy, ν_0 is attempt frequency, and T_0 is Vogel-Fulcher temperature. By imposing $g(\tau, T) d(\ln \tau) = f(U_c) dU_c$, we can derive a distribution function of activation energy barriers.

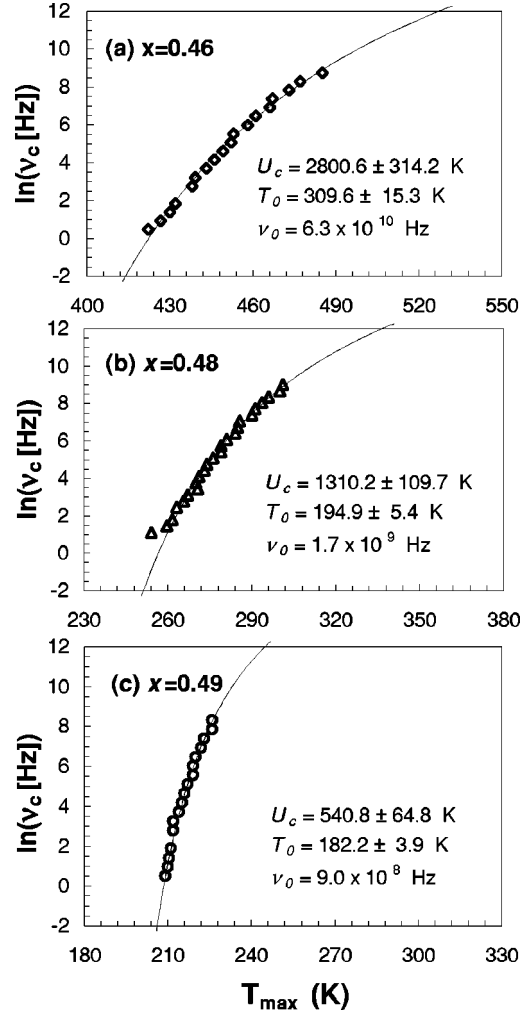


FIG. 2. Cutoff frequency ν_c as a function of T_{max} , the temperature of maximum ϵ'' , for (a) $x=0.46$, (b) $x=0.48$, and (c) $x=0.49$. The solid lines represent the best fit curves of $\nu_c(T_{max})$ to the Vogel-Fulcher law of Eq. (2).

In Fig. 2 the measured frequencies (ν_c) as a function of the maximum ϵ'' -peak temperature (T_{max}) were plotted for each composition. In the case of $x=0.46$, the maximum ϵ'' is not distinct but affected by both the ferroelectric phase transition and the increasing conductivity as shown in Fig. 1(b). For an accurate determination of T_{max} , a peak structure of ϵ'' was deconvoluted by the best-fit Lorentzian distribution functions (see Appendix B). The frequency dispersion in the

TABLE I. Best-fit parameters obtained from fitting $\nu_c(T_{max})$ of $\epsilon''(T; \nu)$ by the Vogel-Fulcher law and MPB transition temperatures (T_L).

x	0.46	0.48	0.49
T_L (K)	~ 490	~ 325	~ 235
U_c (K)	2800.6 ± 314.2	1310.2 ± 109.7	540.8 ± 64.8
T_0 (K)	309.6 ± 15.3	194.9 ± 5.4	182.2 ± 3.9
ν_0 (Hz)	6.3×10^{10}	1.7×10^9	9.0×10^8
τ_0 (sec)	2.5×10^{-12}	9.5×10^{-11}	1.8×10^{-10}

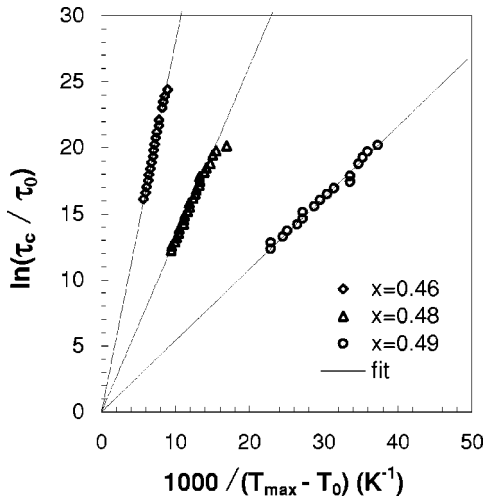


FIG. 3. Vogel-Fulcher plots of relaxation time ($\tau_c = 1/2\pi\nu_c$) against inverse temperature for (\diamond) $x=0.46$, (\triangle) $x=0.48$, and (\circ) $x=0.49$ in $\text{Pb}(\text{Zr}_{1-x}\text{Ti}_x)\text{O}_3$ thin films. The solid lines are the best fits with the three parameters $\nu_0 = 1/2\pi\tau_0$, T_0 , and U_c .

$x=0.49$ sample is relatively narrow. The dielectric dispersion data are well fitted to the Vogel-Fulcher (VF) law except for a small deviation in the low frequency side. The parameters evaluated from the best fits are summarized in Table I. The freezing temperatures (T_0) are 309.6 ± 15.3 K, 194.9 ± 5.4 K, and 182.2 ± 3.9 K for $x=0.46$, 0.48 , and 0.49 , respectively. Both the activation energy (U_c) and the attempt frequency (ν_0) can be seen to decrease as the concentration (x) is increased. A Vogel-Fulcher plot of the relaxation times ($\tau_c = 1/2\pi\nu_c$) is redrawn in Fig. 3 to depict a

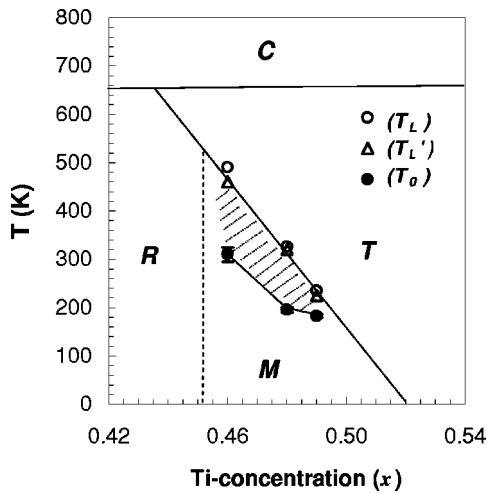


FIG. 4. x - T phase diagram in the vicinity of the MPB for $\text{Pb}(\text{Zr}_{1-x}\text{Ti}_x)\text{O}_3$ thin films. The data points represent, (\bullet) the VF freezing temperatures T_0 , and (\circ) the MPB transition temperatures T_L and (\triangle) T'_L obtained from dielectric measurements and switching current data, respectively. The shaded region indicates the frequency dispersion region. The phase boundaries are indicated by guide lines from other references (see text and Ref. 27) with C, T, M, and R representing cubic, tetragonal, monoclinic, and rhombohedral phases, respectively.

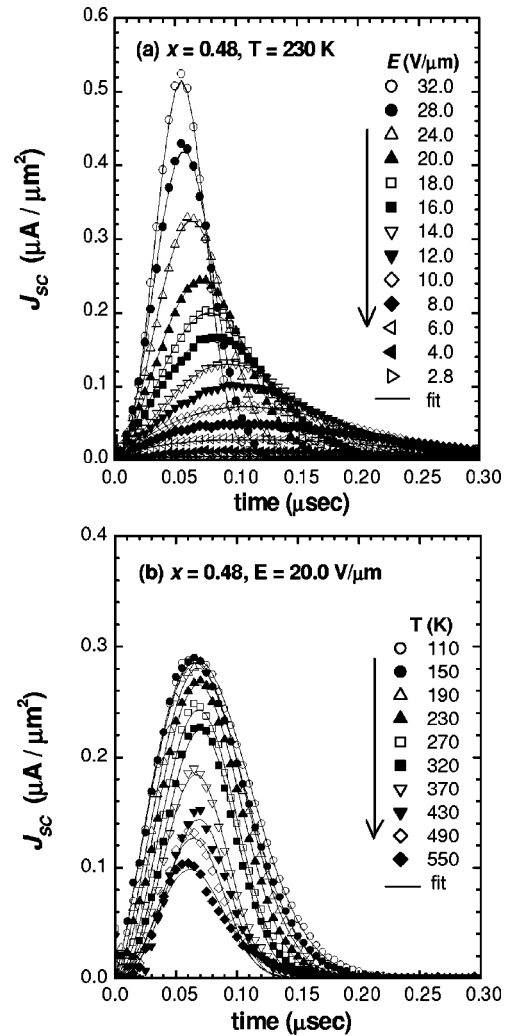


FIG. 5. Switching current transients observed in $\text{Pb}(\text{Zr}_{1-x}\text{Ti}_x)\text{O}_3$ thin films ($x=0.48$): (a) at 230 K with varying electric field, and (b) at 20.0 $\text{V}/\mu\text{m}$ with varying temperature. The solid lines represent the best fits to the model of Eq. (5). The arrows show a corresponding guidance to switching current data curves in the directions of (a) decreasing field and (b) increasing temperature.

scaling behavior. The data set on the lines implicate a good Vogel-Fulcher scaling with the best-fit parameters as scaling variables.

Considering the MPB relaxations governed by the Vogel-Fulcher law, one can expect that the frequency dispersion may be limited to a region between the MPB transition temperature (T_L) and the freezing temperature (T_0). The frequency dispersion may be ascribed to a phase coexistence. Then we can expect that the coexistence of the tetragonal and monoclinic (or rhombohedral) phases may be also limited to the same region between the MPB transition temperature (T_L) and the freezing temperature (T_0). Figure 4 shows an experimental phase diagram near the MPB of the PZT thin films. The T_L and T_0 obtained in this study are collected in the x - T phase diagram. The boundary lines of the frequency dispersion region between T_L and T_0 (shaded region) are not parallel to the MPB but can be seen to become nar-

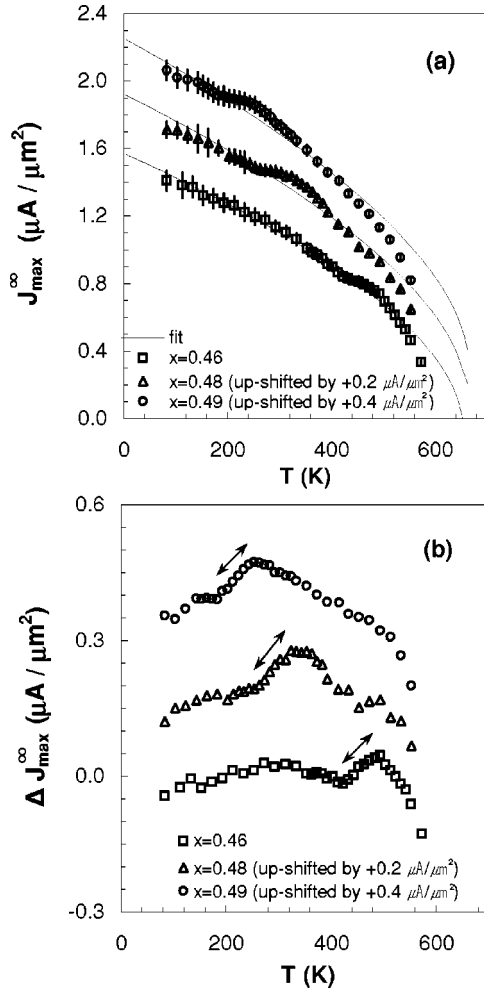


FIG. 6. (a) Temperature dependence of J_{max}^{∞} , the maximum switching current density in the infinite field limit. Solid lines are the best fits by $J_{max}^{\infty}(T) = a|T_C - T|^{\beta/\gamma}$ with $T_C = 660$ K. (b) Deviation of J_{max}^{∞} (experimental data) from the theoretical fit based on the order parameter polarization anomaly. Both J_{max}^{∞} and ΔJ_{max}^{∞} are shifted to avoid overlap confusions by $+0.2$ and $+0.4 \mu\text{A}/\mu\text{m}^2$ for (Δ) $x=0.48$ and (\circ) $x=0.49$, respectively.

rower with increasing concentration (x). For the PZT ceramics, the phase coexistence region suggested by Zhang *et al.*⁷ is parallel to the MPB with a width of ~ 110 K while the one by Noheda *et al.*¹¹ has the shape of a right-angle triangle.¹¹ The frequency dispersion region in our phase diagram for the PZT thin films is a hybrid of the above two results of the phase coexistence region. This similarity between the phase coexistence regions and the frequency dispersion region suggests a close relation between the two.

Although the results reflect a glassy behavior of dipole glasses^{16–18} or ferroelectric relaxors,^{19,20} there is a distinct difference. A polarization order parameter exists in the frequency dispersion region such as that of the $[\text{PMN}]_{0.67}[\text{PT}]_{0.33}$ single-crystal system.¹⁴ The frequency dispersions may be caused by random interactions between two types of randomly distributed ferroelectric clusters with tetragonal and monoclinic (or rhombohedral) symmetries. A random distribution of the two types of polar clusters may

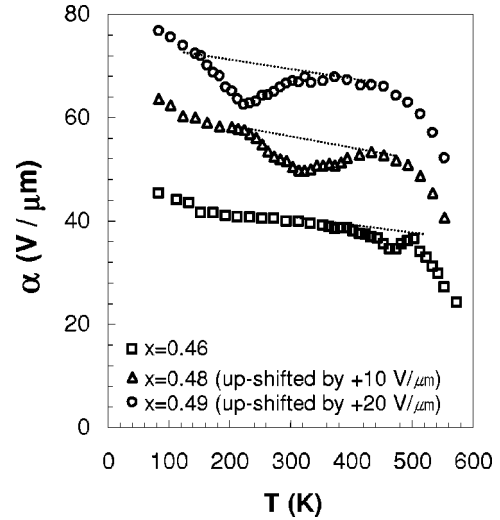


FIG. 7. Temperature dependence of activation field α obtained from fitting $J_{max}(E, T)$ to Eq. (6). α data sets are shifted to avoid overlaps by $+10$ and $+20 \text{ V}/\mu\text{m}$ for (Δ) $x=0.48$ and (\circ) $x=0.49$, respectively. The dotted lines are guides to the eyes.

bring about short-range ordering in competition with long-range ordering.

B. Switching characteristics

In Fig. 5 typical switching current transients in an $x=0.48$ sample are shown at 230 K with varying applied electric field [Fig. 5(a)], and at $20.0 \text{ V}/\mu\text{m}$ with varying temperature [Fig. 5(b)]. A switching current [$J_{SC}(t)$] was obtained by subtracting a nonswitching current [$J_{NS}(t)$] from a full current [$J_{FC}(t)$]. Switching characteristics related to the domain reversal kinetics of ferroelectric systems have been successfully described by Ishibashi and Takagi²¹ based on the Johnson, Mehl, and Avrami model:^{22–24}

$$J_{SC}(t) = J_{FC}(t) - J_{NS}(t) = \frac{dP(t)}{dt} = 2P_s \frac{dQ(t)}{dt}, \quad (3)$$

where P_s represents saturation polarization at long times or high fields and $Q(t)$ is the fraction of switched volume at time t . In general, the nucleation time is very short—several nanoseconds in ferroelectric thin films. Therefore, assuming that domains may grow at a fixed velocity after the nucleation, the fraction of the switched volume can be written as

$$Q(t) = 1 - \exp[-(t/t_0)^n], \quad (4)$$

where n is an effective dimension and t_0 is a characteristic time. The current density due to the domain switching is thus given as

$$J_{SC}(t) = 2P_s(n/t_0)(t/t_0)^{n-1} \exp[-(t/t_0)^n]. \quad (5)$$

In Fig. 5 the experimental data were fitted by Eq. (5) to obtain three parameters, P_s , t_0 , and n . From each best fit we

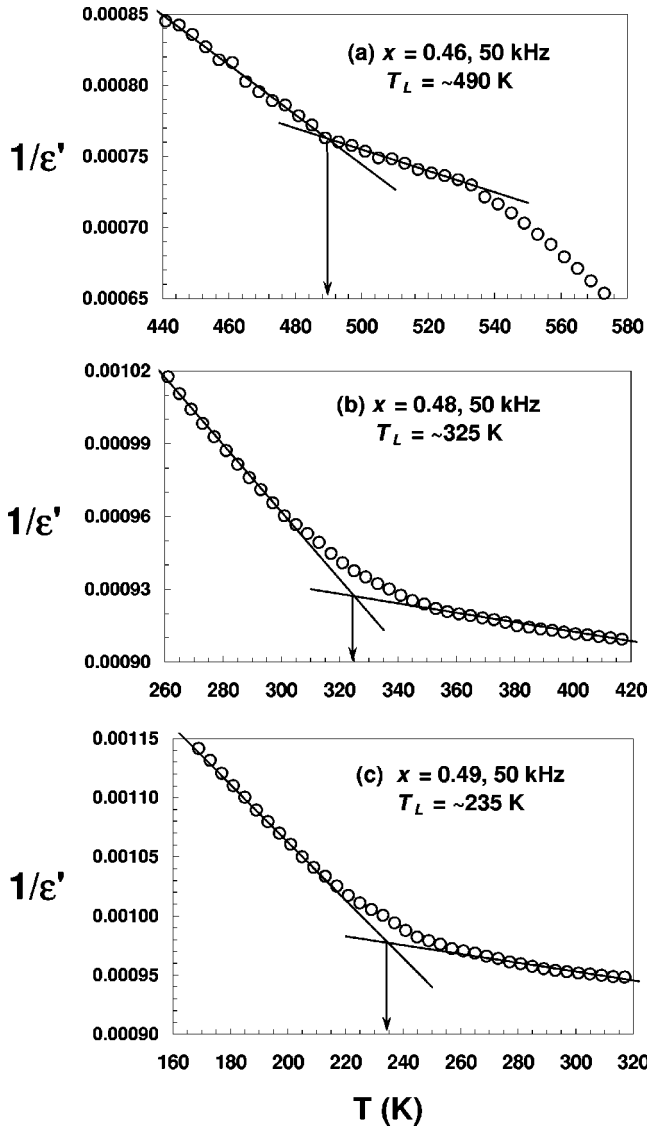


FIG. 8. Determination of the MPB transition temperatures (T_L) from ϵ' data measured at 50 kHz for (a) $x=0.46$, (b) $x=0.48$, and (c) $x=0.49$. The solid lines represent best-fit linear slopes.

could also obtain maximum switching current density (J_{max}), times of maximum switching current density (t_{max}), and switching time (t_{sw}). At higher fields and higher temperatures, the switching current curve can be seen to have shorter switching times and symmetric forms.

Switching current transients were measured at electric fields from $2 \text{ V}/\mu\text{m}$ to $32 \text{ V}/\mu\text{m}$ with varying temperature for all three samples of $x=0.46$, 0.48 , and 0.49 . All the data of switching currents were fitted by Eq. (5). The results show that the effective dimension (n) increases from 1.0 to 2.5, and the characteristic time (t_0) decreases with increasing field or increasing temperature. Unlike the [PMN]- x [PT] or PMN crystal system,¹⁴ an abrupt step change or a plateau behavior in the temperature dependence of polarization was not observed in the PZT thin films of the present work. In the PZT thin-film systems, in fact, it was difficult to obtain reliable saturation polarizations at high fields due to dielectric breakdown. Therefore, an alternative to the saturation polarization should be considered.

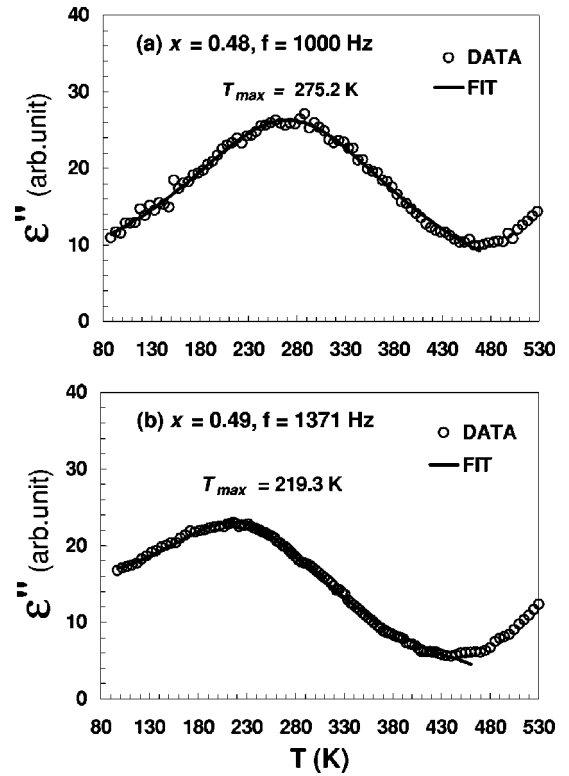


FIG. 9. Determination of the maximum peak temperature (T_{max}) of $\epsilon''(T)$ for (a) $x=0.48$ and (b) $x=0.49$. The solid line represents a Lorentzian function best fit by Eq. (B1).

The maximum switching current density (J_{max}) and the switching time (t_{sw}) as a function of the applied field (E) follow the well-known empirical laws²⁵

$$J_{max}(E, d, T) = J_{max}^{\infty}(d, T) \exp[-\alpha(d, T)/E], \quad (6)$$

$$t_{sw}(E, d, T) = t_{sw}^{\infty}(d, T) \exp[\alpha(d, T)/E], \quad (7)$$

where $\alpha(d, T)$ is the activation field dependent on thickness (d) and temperature (T), and $J_{max}^{\infty}(d, T)$ and $t_{sw}^{\infty}(d, T)$ are the maximum switching current and switching time, respectively, in the limit of infinite electric field. $J_{max}^{\infty}(d, T)$ of the high-field limit is related to the saturation polarization.

The temperature dependence of $J_{max}^{\infty}(T)$ is shown for $x=0.46$, 0.48 , and 0.49 in Fig. 6(a) (for a clear view of comparisons, the data of $x=0.48$ and 0.49 are shifted each by $+0.2$ and $+0.4 \mu\text{A}/\mu\text{m}^2$, respectively). $J_{max}^{\infty}(T)$, the maximum switching current density at infinite electric field, shows a plateau near the MPB transition with a smooth temperature dependence for all three compositions. Since $J_{max}^{\infty}(T)$ is associated with the saturation polarization at high fields, $J_{max}^{\infty}(T)$ may be a substitute for an order parameter. Although the ferroelectric transition of the PZT system is familiar as a first-order phase transition, we may attempt to fit the data by $J_{max}^{\infty}(T) \sim P_s^{1/\gamma} \sim a|T_C - T|^{\beta/\gamma}$ to embody the anomalies. With $T_C=660 \text{ K}$ and the best-fit exponent $\beta/\gamma = 0.575$, 0.588 and 0.603 for each system of $x=0.46$, 0.48 ,

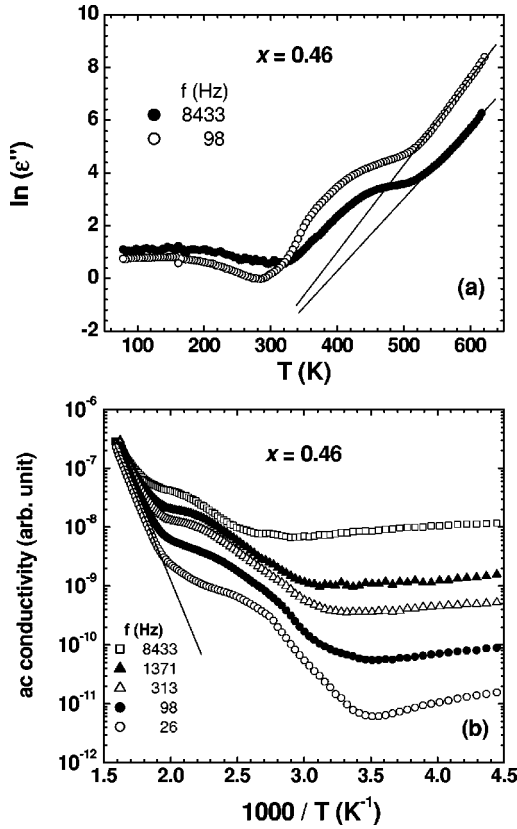


FIG. 10. Logarithmic plots of $\epsilon''(T)$ data for $x=0.46$: (a) $\ln(\epsilon'')$ vs temperature, and (b) ac conductivity vs inverse temperature. The solid lines represent best fits by $\exp(aT+b)$ in (a) and $\exp(-a/T+b)$ in (b).

and 0.49, respectively, we examined deviations of the data $J_{max}^{\infty}(T)$ from each phase-transition curve of the theoretical best fits. This deviation from the phase-transition anomaly is seen to increase near the MPB and in the high temperature region. Difference between data and each best-fit curve, $\Delta J_{max}^{\infty}(T)$, is plotted in Fig. 6(b). Anomalies of $J_{max}^{\infty}(T)$ near the MPB transitions can be seen to be pronounced. The arrow-marked region in a broad peak of $\Delta J_{max}^{\infty}(T)$ corresponds to the plateau anomaly region of $J_{max}^{\infty}(T)$ in Fig. 6(a). The anomalies are continuous at the MPB. The saturation polarization at high fields may have a similar plateau anomaly of a smooth temperature dependence near the MPB. For $x=0.46, 0.48,$ and 0.49 , the temperatures of the plateau anomalies in $J_{max}^{\infty}(T)$ are found to be in the ranges of 435 ~ 490 K, 275 ~ 335 K, and 200 ~ 245 K, respectively. These temperature ranges include the MPB transition temperatures (T_L) obtained from the dielectric constant data at 50 kHz for the respective compositions.

Figure 7 shows temperature dependence of the activation field (α) for each composition (for a clear comparison, the data curves for $x=0.48$ and 0.49 are upshifted each by +10 and +20 V/ μm , respectively). $\alpha(T)$ exhibits a broad dip around the MPB transition. Temperatures of minimum α in each dip can be located at ~ 460 K, ~ 320 K, and ~ 225 K for $x=0.46, 0.48$ and 0.49 , respectively. They are close to the MPB transition temperatures obtained from the measure-

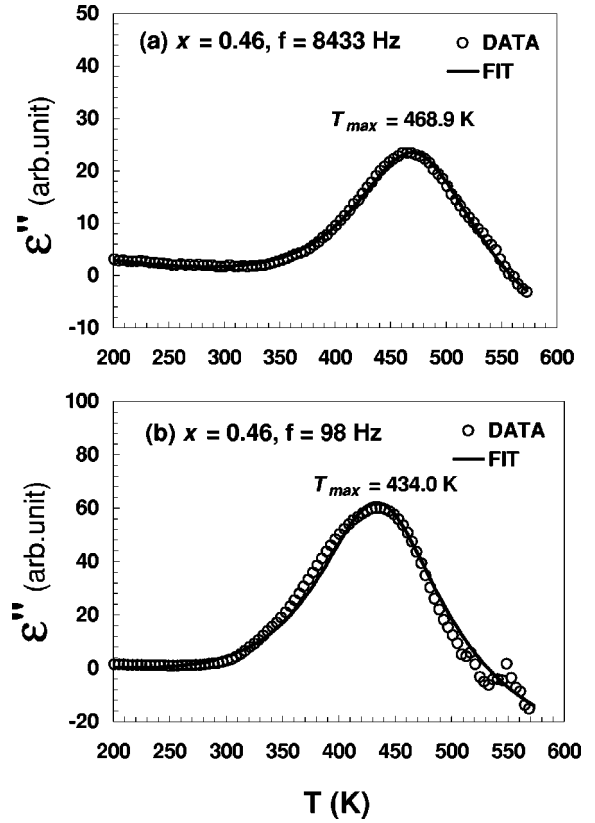


FIG. 11. Determination of the maximum peak temperatures (T_{max}) of $\epsilon''(T)$ for $x=0.46$ at (a) 8433 Hz and (b) 98 Hz. The solid line represents a Lorentzian function best fit by Eq. (B1).

ments of dielectric constants at 50 kHz for the respective compositions. The minimum dip temperatures (T_L') are denoted by Δ symbols in Fig. 4. Reduction of the activation field near the MPB implies that the polarization domain reversal becomes easier with a shorter tail of polarization switching. In the vicinity of the MPB, random fluctuations of polar directions can be caused by nearly isotropic free energy²⁶ as well as the phase coexistence. These additional degrees of rotational freedom^{2,26} in polar directions may well reduce the effective activation field for domain reversals.

IV. CONCLUSIONS

Temperature dependencies of dielectric constants and switching properties of the $\text{Pb}(\text{Zr}_{1-x}\text{Ti}_x)\text{O}_3$ thin films were investigated in the range of 80 ~ 600 K to analyze anomalies near the morphotropic phase boundary. In the $\text{Pb}(\text{Zr}_{1-x}\text{Ti}_x)\text{O}_3$ thin films of $x=0.46, 0.48,$ and 0.49 , we could observe anomalies in both ϵ' and ϵ'' near the MPB transition. The anomalies of the MPB exhibit a frequency dispersion and tend to a low-temperature phase transition. We have found that the frequency dispersion of the ϵ'' peaks near the MPB follows the Vogel-Fulcher law. The frequency dispersion in the region between the MPB transition and the freezing temperature may be ascribed to coexistence of tetragonal and monoclinic (or rhombohedral) phases. This phase coexistence region for the PZT thin films has a form between parallel columnar and the right-angle triangle re-

ported for the PZT ceramics. The switching current transient of polarization reversal could be characterized by the Ishibashi model. The maximum switching current density in the infinite field limit, which is associated with the saturation polarization, has a plateau anomaly near the MPB transition. Reduction of activation fields for polarization reversals near the MPB transition was found, which may be ascribed to increasing fluctuations due to phase coexistence and a rotational random distribution of polar directions at the MPB.

ACKNOWLEDGMENTS

This work was supported in part by the KAIST Chair Fund endowed from Korea Telecom.

APPENDIX A: DETERMINATION OF T_L

Real part dielectric constant (ϵ') data measured at 50 kHz are plotted in the plane of inverse dielectric constant ($1/\epsilon'$) versus temperature (T) in Fig. 8, where the best-fit extrapolations of the changing slopes locate crossover points to define the MPB transition temperatures within the error bars of ~ 20 K.

APPENDIX B: DETERMINATION OF T_{max}

For $x=0.48$ and $x=0.49$ the raw data of $\epsilon''(T)$ were best fitted directly by the following Lorentzian function:

$$\epsilon''(T) = \frac{\epsilon''_{peak}}{1 + [(T - T_{max})/\Gamma_{peak}]^2} \quad (\text{B1})$$

to obtain T_{max} as shown in Fig. 9. However, for $x=0.46$ the ϵ'' peak of the MPB is strongly influenced by increasing conductance and ferroelectric transition. Since our concern is only with T_{max} , we redraw our raw data in a logarithmic scale as shown in Fig. 10. This log plot exhibits a linear dependence region at high temperatures. These linear regions can be fitted by $\exp(aT+b)$ and $\exp(-a/T+b)$ to obtain the best-fit values of a and b . We then subtract these contributions of $\exp(aT+b)$ or $\exp(-a/T+b)$ from the corresponding raw data to obtain genuine peak anomalies as shown in Fig. 11, where we apply the Lorentzian function best fits of Eq. (B1) to determine T_{max} .

*Electronic address: jjkim@cais.kaist.ac.kr

¹S.-E. Park and T. R. ShROUT, J. Appl. Phys. **82**, 1804 (1997).

²H. Fu and R. E. Cohen, Nature (London) **403**, 281 (2000).

³D. E. Cox, B. Noheda, G. Shirane, Y. Uesu, K. Fujishiro, and Y. Yamada, Appl. Phys. Lett. **79**, 400 (2001).

⁴S. Kim, I.-S. Yang, J.-K. Lee, and K. S. Hong, Phys. Rev. B **64**, 094105 (2001).

⁵S. K. Mishra, D. Pandey, and A. P. Singh, Appl. Phys. Lett. **69**, 1707 (1996).

⁶S. K. Mishra and D. Pandey, J. Phys.: Condens. Matter **7**, 9287 (1995).

⁷S. Zhang, X. Dong, and S. Kojima, Jpn. J. Appl. Phys., Part 1 **36**, 2994 (1997).

⁸A. G. S. Filho, K. C. V. Lima, A. P. Ayala, I. Guedes, P. T. C. Freire, J. M. Filho, E. B. Araujo, and J. A. Eiras, Phys. Rev. B **61**, 14 283 (2000).

⁹Ragini, S. K. Mishra, D. Pandey, H. Lemmens, and G. V. Tendeloo, Phys. Rev. B **64**, 054101 (2001).

¹⁰B. Noheda, D. E. Cox, G. Shirane, J. A. Gonzalo, L. E. Cross, and S.-E. Park, Appl. Phys. Lett. **74**, 2059 (1999).

¹¹B. Noheda, D. E. Cox, G. Shirane, R. Gou, B. Jones, and L. E. Cross, Phys. Rev. B **63**, 014103 (2000).

¹²L. Bellaiche, A. Garcia, and D. Vanderbilt, Phys. Rev. Lett. **84**, 5427 (2000).

¹³V. Y. Topolov and A. V. Turik, J. Phys.: Condens. Matter **13**, L771 (2001).

¹⁴V. H. Schmidt, C.-S. Tu, C.-H. Yeh, H. Luo, and F.-C. Chao, in *Fundamental Physics of Ferroelectrics 2000*, edited by Ronald E. Cohen, AIP Conf. Proc. No. 535 (AIP, Melville, NY, 2000), p. 240.

¹⁵E. Courtens, Phys. Rev. B **33**, 2975 (1986).

¹⁶B.-G. Kim and J.-J. Kim, Phys. Rev. B **55**, 5558 (1998).

¹⁷E. Courtens, Phys. Rev. Lett. **52**, 69 (1984).

¹⁸Z. Kutnjak, C. Fillipic, A. Levstik, and R. Pirc, Phys. Rev. Lett. **70**, 4015 (1993).

¹⁹A. Levstik, Z. Kutnjak, C. Fillipic, and R. Pirc, Phys. Rev. B **57**, 11 204 (1998).

²⁰A. E. Glazounov and A. K. Tagantsev, Appl. Phys. Lett. **73**, 856 (1998).

²¹Y. Ishibashi and Y. Takagi, J. Phys. Soc. Jpn. **31**, 506 (1971).

²²T. D. User, C. P. Poole Jr., and H. A. Farach, Ferroelectrics **120**, 201 (1991).

²³J. F. Scott, L. Kammerdiner, M. Parris, S. Traynor, V. Ottenbacher, A. Shawabkeh, and W. F. Oliver, J. Appl. Phys. **64**, 787 (1988).

²⁴K. Matyjasek, J. Phys. D **34**, 2211 (2001).

²⁵W. J. Merz, Phys. Rev. **95**, 690 (1954).

²⁶M. Iwata, H. Orihara, and Y. Ishibashi, Jpn. J. Appl. Phys., Part 1 **40**, 708 (2001).

²⁷B. Jaffe, W. R. Cook, and H. Jaffe, *Piezoelectric Ceramics* (Academic, London, 1971).